Eur. Phys. J. E (2009)
DOI 10.1140/epje/i2009-10511-x

THE EUROPEAN PHYSICAL JOURNAL E

Regular Article

Gallium nitride electrodes for membrane-based electrochemical biosensors

T. Schubert[1], G. Steinhoff[2], H.-G. von Ribbeck[2], M. Stutzmannn[2], M. Eickhoff[3], and M. Tanaka[1,a]

[1] Institut für Physikalische Chemie, Universität Heidelberg, Im Neuenheimer Feld 253, 69120 Heidelberg, Germany
[2] Walter Schottky Institut, Technische Universität München, Am Coulombwall, 85748 Garching, Germany
[3] I. Physikalisches Institut, Justus-Liebig-Universität Giessen, Heinrich-Buff-Ring 16, 35392 Giessen, Germany

Received 11 March 2009 and Received in final form 27 April 2009

Abstract. We report on the deposition of planar lipid bilayers (supported membranes) on gallium nitride (GaN) electrodes for potential applications as membrane-based biosensors. The kinetics of the lipid membrane formation upon vesicle fusion were monitored by simultaneous measurements of resistance and capacitance of the membrane using AC impedance spectroscopy in the frequency range between 50 mHz and 50 kHz. We could identify a two-step process of membrane spreading and self-healing. Despite its relatively low resistance, the membrane can be modeled by a parallel combination of an ideal resistor and capacitor, indicating that the membrane efficiently blocks the diffusion of ions.

PACS. 84.37.+q Measurements in electric variables (including voltage, current, resistance, capacitance, inductance, impedance, and admittance, etc.) – 87.14.Cc Lipids – 87.85.fk Biosensors

1 Introduction

Functional coupling of biological systems to electronic transducers draws increasing attention to the creation of hybrid biosensors, which sensitively translate specific functions of biomolecules into electrical signals. In nature, numerous specific recognition processes take place in cell membranes based on integral and peripheral membrane proteins. Thus, the deposition of biomembranes [1–4] on solid-state electronic devices is the first step to achieve immobilization of membrane proteins without denaturation. Compared to metal electrodes, the use of semiconductors is advantageous due to the capability to control their electronic properties by doping, to fabricate heterostructures (band-gap engineering), and the possibility of realizing parallel, multimodal optical/electrical sensing [5]. The favored device platform for such applications is the field-effect transistor (FET) [6], which has been applied to different systems, including covalently anchored DNA [7], enzymes [8], and cells [9]. Another approach with less device complexity is to use larger electrodes as conductive [10,11] or capacitive sensors [12,13]. In the most frequently used Si-based devices, hydrophilic Si/SiO_2 semiconductor/oxide structures have been used as sensors in aqueous environments for instance to detect the electrical activity of living cells [9,14] as well as for supported lipid membranes incorporating ion channel proteins [11]. However, silicon-based devices suffer from their limited chemical stability in physiological buffers [15].

To overcome this chemical instability, the group-III nitride material system has recently received a lot of attention for the application in biochemical sensors [16–21]. GaN is especially promising as it is a wide-band semiconductor (*i.e.* transparent to visible light) and possesses excellent chemical robustness. In previous works, it was demonstrated that GaN has a high *p*H sensitivity of 57.3 mV/*p*H [22], and we succeeded in the deposition of uniform, freely diffusive supported membranes on GaN [5]. The chemical functionalization of GaN surfaces can be achieved by covalent coupling of organic silanes [16] which can further be used for controlled covalent coupling of enzymes and the electronic detection of their catalytic activity [23]. In another study, we have successfully detected cellular action potentials with AlGaN/GaN field-effect transistors [24].

In this study, Si-doped GaN layers on *c*-plane sapphire substrates, grown by metal organic chemical vapour deposition (MOCVD) were used to investigate the electrical properties of supported lipid membranes on GaN electrodes.

2 Materials and methods

2.1 Gallium nitride substrates

GaN films with (0001)-orientation grown on *c*-plane sapphire substrates with a total thickness of 2.9 μm were used

[a] e-mail: tanaka@uni-heidelberg.de

Published online: 03 September 2009

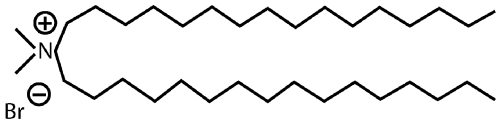

Fig. 1. The structure of 1,2-dihexadecyl-dimethylammonium bromide (DHDAB).

as electrode material. The GaN electrodes were grown by metal organic chemical vapour deposition (MOCVD) (TopGaN, Warsaw, Poland). The topmost layer was a 250 nm thick Si-doped ($2 \times 10^{19}\,\mathrm{cm}^{-3}$) GaN film. Prior to deposition of lipid bilayers, the samples were cleaned with organic solvents and then subjected to a wet chemical surface treatment in a 3:1 mixture of H_2SO_4/H_2O_2 to achieve hydrophilic surfaces, as described in previous work [16].

2.2 Chemicals and lipid membrane preparation

The buffer used was phosphate buffered saline (PBS) at *p*H 7.0, containing 10 mM NaH_2PO_4/Na_2HPO_4 and 50 mM NaCl. Before electrochemical experiments, the buffer was degassed. Supported membranes consist of 60 mol% of positively charged 1,2-dihexadecyl-dimethylammonium-bromide (DHDAB, Fig. 1) and 40 mol% cholesterol (Avanti Polar Lipids AL, USA) to achieve a high electrical membrane resistance [11]. A mixture of lipid and cholesterol was dried from chloroform solution under a stream of nitrogen and stored in vacuum overnight to remove traces of solvents. Then the lipid film was resuspended in buffer at a concentration of 1 μM/ml and incubated at 40 °C for 2 h. Afterwards, the lipid suspension was sonicated with a tip sonifier for 15 min until a clear solution was obtained. Finally, the solution was centrifuged to remove titanium particles. This vesicle suspension (1 μM/ml) was injected into the flow chamber and incubated at room temperature to spread a supported lipid membrane on the hydrophilic surface prepared by the wet chemical treatment.

2.3 Electrochemical methods

Electrochemical experiments were performed in a flow chamber in a three-electrode configuration. A GaN serves as the working electrode and a platinum wire as the counter electrode. All potentials were measured against a Ag/AgCl reference electrode (Metrohm, Filderstadt, Germany). Due to the insulating sapphire carrier substrate, the GaN electrodes were contacted with spring-loaded pins outside the chamber from the front side onto four Ti (30 nm)/Au (100 nm) Ohmic contacts. Since the contact area is sufficiently large, Ohmic contacts could be realized without an additional annealing step. The chamber was sealed with an o-ring, leaving an active area of $0.128\,\mathrm{cm}^2$. The buffer solution was continuously pumped through the chamber with a peristaltic pump (ISMATEC, Glattburg, Austria). The electrochemical cell was placed in a dark shielded Faraday cage during experiments.

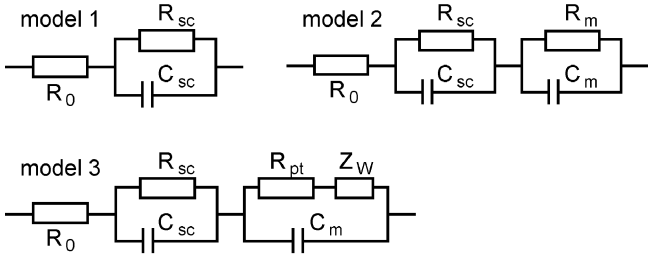

Fig. 2. Equivalent-circuit models used in this study. Models 1 and 2 include only ideal resistors and capacitors, while model 3 includes a Warburg element.

Impedance measurements were performed with a VoltaLab 40 (Radiometer Analytical). A 750 Ω resistance was inserted in series with the GaN electrode to improve the high-frequency signal. Spectra were recorded with an AC amplitude of 20 mV within the frequency range between 50 mHz and 50 kHz.

The electrical properties of the GaN electrode and of the lipid membranes were extracted by modeling the impedance spectra with the equivalent circuits depicted in Figure 2. Model 1 contains a series combination of a resistance R_0 representing the Ohmic characteristics of contact wires and electrode and a parallel circuit of resistance and capacitance to model the semiconductor interface. Model 2 contains an additional ideal RC element to model the resistance R_m and the capacitance C_m of the supported membrane. In model 3, the membrane resistance is represented by a serial connection of a Warburg element Z_W and a phase transfer resistance R_pt to account for diffusion-barrier properties of the membrane [25,26].

3 Results

3.1 Characterization of bare GaN electrodes

Prior to membrane deposition, the electrochemical properties of the bare GaN electrodes were characterized by impedance spectroscopy at $V_\mathrm{bias} = 0\,\mathrm{V}$ (Fig. 3). As can be seen, the data can be fitted well with model 1. Similar to our previous studies on GaAs [27,28], no contribution from surface states can be detected by impedance measurements in the frequency range between $f = 50\,\mathrm{mHz}$ and 50 kHz and $V_\mathrm{bias} = -0.3 \div +1.5\,\mathrm{V}$. Thus, the interface capacitance $C_\mathrm{sc} = 0.8\,\mu\mathrm{F/cm}^2$ calculated with model 1 is dominated by the capacitance of the GaN space charge region. It should also be noted that the electrode interface resistance R_sc is so high that only its lower limit ($R_\mathrm{sc} > 10\,\mathrm{M\Omega\,cm}^2$) can be determined within the examined frequency range.

Figure 4 represents the calculated values for $1/C_\mathrm{sc}^2$ plotted as a function of the applied bias potentials V_bias (Mott-Schottky plot). Assuming an ideal Schottky barrier at the electrolyte/GaN interface, the relationship between

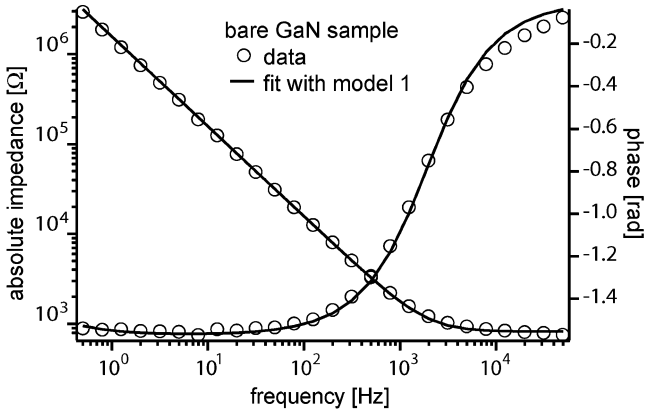

Fig. 3. Absolute impedance and phase shift (Bode plot) of a bare GaN sample in contact with the buffer at $V_{\mathrm{bias}} = 0\,\mathrm{V}$. Circles are the measured data points, while the solid lines represent the fit results using model 1.

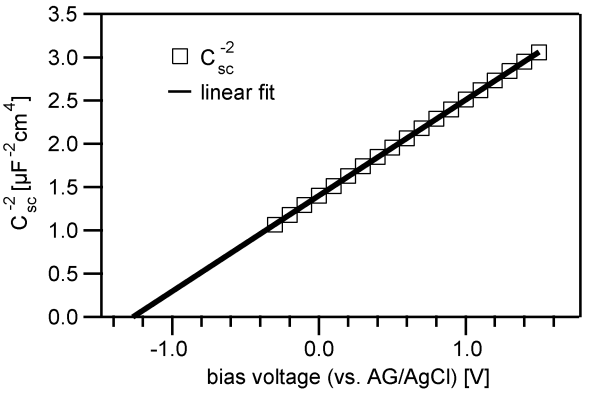

Fig. 4. Mott-Schottky plot ($1/C_{\mathrm{sc}}^2$ *vs.* V_{bias}) of a bare GaN electrode, obtained by measuring the interface capacitance C_{sc} at various bias potentials. The intercept of the linear extrapolation with the x-axis yields a flat-band potential of $V_{\mathrm{fb}} = -1.3\,\mathrm{V}$.

the depletion layer capacitance C_{sc} and V_{bias} is described by

$$\frac{1}{C_{\mathrm{sc}}^2} = \frac{2}{eN_{\mathrm{D}}\varepsilon_{\mathrm{sc}}\varepsilon_0}\left[(V_{\mathrm{bias}} - V_{\mathrm{fb}}) - \frac{kT}{e}\right], \qquad (1)$$

where N_{D} is the doping concentration, V_{fb} is the flat-band potential, and the other constants have their usual meanings. The intersection of the linear extrapolation with the x-axis yields the flat-band potential $V_{\mathrm{fb}} = -1.3\,\mathrm{V}$. From the slope of the plot, the concentration of ionized donors in the semiconductor [29,30] $N_{\mathrm{D}} = (1.2 \pm 0.1) \times 10^{19}\,\mathrm{cm}^{-3}$ can be calculated, in agreement with results from Hall-effect measurements. Furthermore, no indication of an electrical contribution of surface states or surface layers is noticed in the impedance spectra and the Mott-Schottky plots are linear. This observation confirms that the observed voltage-dependent interface capacitance C_{sc} is dominated by the behavior of the semiconductor depletion layer. The GaN electrodes show no sign of irreversible drift or electrochemical degradation throughout the experiments performed at wide frequency and bias potential ranges, confirming the chemical robustness of GaN for electrochemical sensing in physiological buffers.

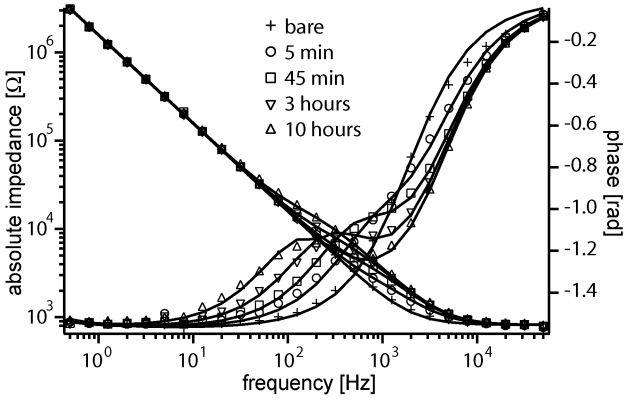

Fig. 5. Impedance spectra recorded during formation of a lipid membrane on a GaN electrode. Fits are made according to model 2.

3.2 Electrochemical monitoring of membrane formation on GaN

The cationic lipid DHDAB in different molar ratios to cholesterol has been shown in prior works to be capable of forming membranes with a very high resistance [11]. Partially this is due to the small headgroup cross-sectional area which allows very tight hydrocarbon chain packing. Also, we have previously shown that membranes of DHDAB are capable of supporting functional transmembrane proteins such as gramicidin [11,31]. While other membrane compositions including phospholipids are possible, for the initial device characterization membranes of DHDAB/cholesterol are ideally suited to highlight the system/substrate performance.

Figure 5 shows the change in impedance spectra of the GaN electrode in contact with the lipid vesicle suspension. A clear change in both absolute impedance and phase shift can be observed already at $t = 5\,\mathrm{min}$ (open circles). The overall shape of the spectra is preserved during the entire duration of the experiment. Washing away supernatant and adsorbed vesicles by vigorous exchange of electrolyte buffer does not lead to any detectable change in the impedance spectrum, clearly suggesting the formation of a highly stable dielectric layer at the GaN/electrolyte interface. In fact, the obtained results can be well represented by the circuit model 2 in Figure 2 (solid lines in Fig. 5).

Figure 6A represents the extracted values for C_{m} and R_{m} as a function of time, reflecting the kinetics of membrane formation. Both C_{m} and R_{m} values show continuous change in a fashion which is understandable in the terms of Langmuir adsorption kinetics. The tendency agrees well with previous results obtained for the deposition of a lipid bilayer on ITO [31] and Si/SiO_2 [11] electrodes. Both resistance and capacitance develop as double exponentials with comparable time-constants for the fast ($\tau_{R,\mathrm{fast}} = 4.1\,\mathrm{min}$, $\tau_{C,\mathrm{fast}} = 5.8\,\mathrm{min}$) and slow ($\tau_{R,\mathrm{slow}} = 50\,\mathrm{min}$, $\tau_{C,\mathrm{slow}} = 57\,\mathrm{min}$) processes. Furthermore, as shown in Figure 6B,

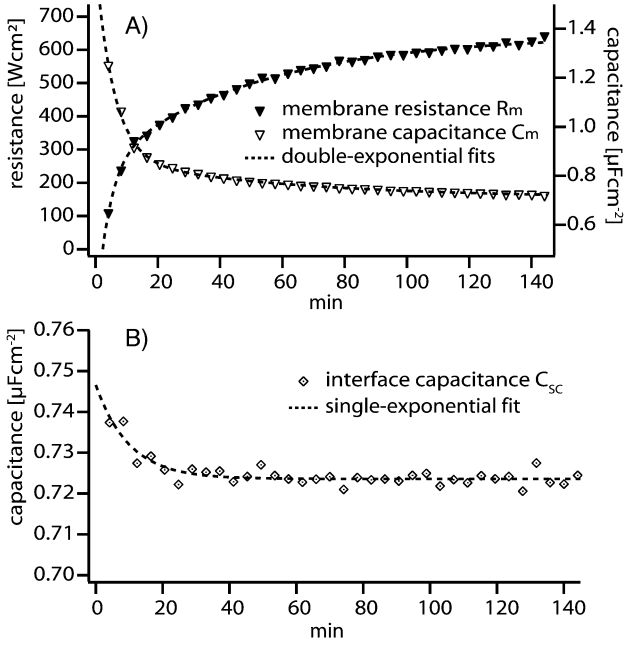

Fig. 6. Kinetics of the formation of a phospholipid membrane on a GaN electrode. Upon the injection of vesicle suspensions, A) the capacitance C_{m} and resistance R_{m} of the membrane show continuous changes (double exponentials), while B) the interface capacitance of the semiconductor C_{sc} remains stable at long times. This confirms that the deposition of lipid membrane does not cause any electrochemical changes of the semiconductor surface.

the semiconductor capacitance C_{sc} shows little change, and can be fitted with a single exponential with a time-constant $\tau_{\mathrm{sc}} = 10\,\mathrm{min}$. Beyond this time frame, the substrate capacitance remains unchanged. The small shift in substrate capacitance can be attributed to a change in the surface potential corresponding to the adsorption of the charged cationic membrane. This does not only give supporting evidence for the chemical robustness of GaN electrodes but also justifies our choice of the circuit model.

Previously, using the surface plasmon resonance and a quartz crystal microbalance, Keller *et al.* [32] proposed that the kinetics of supported membrane formation on a hydrophilic silica surface comprises two steps: i) adsorption of vesicles and ii) spreading on the surface. However, it should be pointed out that electrochemical impedance measurements are not sensitive to the first step, since adherent vesicles do not form a dielectric layer. Membrane adsorption/spreading experiments on comparable systems using AFM or QCMD [33,34] observe saturation at short times, comparable to the fast kinetics reported here. But in contrast to these techniques, impedance spectroscopy measurements are much more sensitive to slow self-healing processes affecting the remaining defects and membrane resistivity [2]. The fast kinetics observed in both the membrane and substrate capacitance development appear to correspond to the adsorption and spreading of the majority of the membrane material, while the slower long-term kinetics reflect self-healing of the local defects in fluid membrane that can only be detected by electrochemical techniques.

4 Discussion

It should be noted that the membrane capacitance $C_{\mathrm{m}} = 0.7\,\mu\mathrm{F/cm^2}$ reached at $t = 10\,\mathrm{h}$ agrees well with that reported for a single lipid bilayer [35–37]. In fact, by assuming the dielectric constant of the hydrocarbon chain region to be $\varepsilon = 2.2$, the thickness d_{H} can be calculated from the capacitance to

$$d_{\mathrm{H}} = \varepsilon_0 \varepsilon / C_{\mathrm{m}} = 1.3\,\mathrm{nm}, \tag{2}$$

where ε_0 is the vacuum permittivity. On the other hand, the maximum membrane resistance R_{m} achieved (at $t > 10\,\mathrm{h}$) was $R_{\mathrm{m}} \sim 1\,\mathrm{k\Omega\,cm^2}$, approximately three orders of magnitude smaller than the value reported for lipid bilayers on a Si/SiO_2 electrode, $R_{\mathrm{m}} \sim 1\,\mathrm{M\Omega\,cm^2}$. Since the resistance of free-standing lipid membranes and membrane patches is about $1\,\mathrm{M\Omega\,cm^2}$, the poor resistance would prohibit sensing of selective transport of ions and charged species. Currently, the significant difference in the membrane resistance observed here can be explained either by i) the topographical roughness or chemical heterogeneity of the electrode, or ii) the poor barrier properties of the membrane.

For example, previous accounts reported that the resistance of the same type of membrane deposited on polycrystalline ITO electrodes is of the order of $1\,\mathrm{k\Omega\,cm^2} \sim 100\,\mathrm{k\Omega\,cm^2}$ [31,38], which can be attributed to the higher roughness of ITO (AFM RMS roughness $\sim 3\,\mathrm{nm}$) compared to SiO_2 (RMS roughness $\sim 0.2\,\mathrm{nm}$) [11]. In fact, once the roughness is reduced by the deposition of a ultrathin polymer interlayer (RMS roughness $< 1\,\mathrm{nm}$), the resistance of the membrane can be as high as $0.5\,\mathrm{M\Omega\,cm^2}$ [10]. In our case, the topographic roughness does not seem to play a major role, since the RMS roughness of the sample after the wet chemical etching is only 0.5 nm (measured by AFM, data not shown). However, contact angle measurements (Supporting Information 1) and scanning tunneling electron microscopy (data not shown) suggest that after the wet chemical oxidation the surface possesses chemical heterogeneity.

To verify the second scenario, we applied circuit model 3 (Fig. 2) to estimate the diffusion constant of ions across the membrane. This circuit model includes a so-called Warburg element and a phase transfer resistance R_{pt}. The Warburg element describes linear diffusion to a semi-infinite plane such as large planar electrodes, which can be used as an approximation to quantify diffusion of ions through the membrane, *i.e.* permeability to the ions. The fit with model 3 results in a Warburg parameter $\sigma = 2.7 \times 10^4\,\mathrm{V\,A^{-1}\,s^{-0.5}\,cm^2}$ and a phase transition resistance of $1\,\mathrm{k\Omega\,cm^2}$. The Warburg parameter σ normalized by area is given by [39]

$$\sigma = \frac{\sqrt{2}RT}{cF^2\sqrt{D}}\,, \tag{3}$$

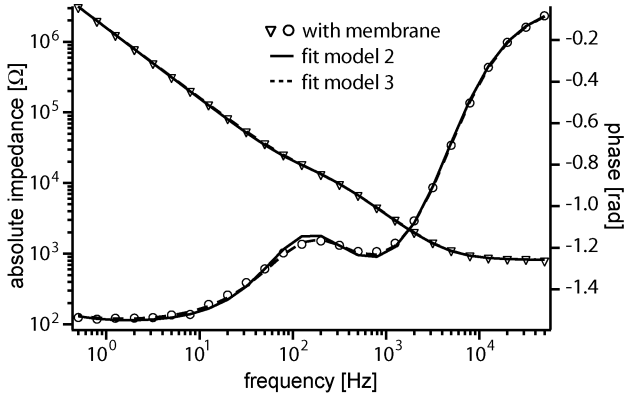

Fig. 7. Comparison of fits with models 2 and 3 of a membrane on GaN. A fit with model 3 (Warburg) shows only a slight improvement over model 2 (ideal elements).

where c is the concentration of the diffusing species, and D is the diffusion coefficient. R, T, and F stand for gas constant, temperature, and Faraday constant, respectively. This leads directly to

$$D = \left[\frac{\sqrt{2}RT}{\sigma c F^2}\right]^2 . \quad (4)$$

From the obtained σ value we calculate a diffusion coefficient for the ions through the membrane of $D \sim 0.02\,\mu\mathrm{m}^2\,\mathrm{s}^{-1}$. This is approximately by a factor of 10^5 times lower than the free diffusion of ions in solution ($D \sim 10^3\,\mu\mathrm{m}^2\,\mathrm{s}^{-1}$), indicating that the membrane can be represented by a RC element despite the poor resistance. Indeed, as presented in Figure 7, the fitting results to the spectra at $t = 10\,\mathrm{h}$ with model 2 (solid line, $\chi^2 = 7.6 \times 10^{-3}$) and model 3 (broken line, $\chi^2 = 1.3 \times 10^{-3}$) show no significant difference.

Thus, it is plausible to attribute the low membrane resistance to point-like defects in the membrane due to chemical heterogeneity of the surface. Furthermore, we performed the same electrochemical experiments on GaN with a higher RMS roughness of $\sim$ 1.5 nm (data not shown). Although the membrane resistance and capacitance are comparable to those on smoother surfaces, the measured spectra can be much better fitted with model 3. This finding suggests that an increased surface roughness reduces the diffusion barrier capability of the membrane.

5 Summary and conclusion

We have demonstrated that gallium nitride (GaN) can be used as a chemically stable platform for membrane-based biosensors. The electrochemical stability of wet chemically oxidized GaN has been demonstrated by electrochemical impedance spectroscopy measurements over wide frequencies and bias potentials, confirming that GaN electrodes can be operated in physiological buffers with no detectable drift or degradation. Lipid bilayer membranes can be deposited on the oxidized GaN, whose electrochemical parameters (resistance and capacitance) can be represented by ideal elements in an equivalent circuit model. The kinetics of the membrane formation can be monitored by plotting the membrane resistance and capacitance as a function of time. Though the calculated membrane capacitance $C_\mathrm{m} = 0.7\,\mu\mathrm{F\,cm}^{-2}$ agrees well with that of a single bilayer membrane, the membrane resistance $R_\mathrm{m} \sim 1\,\mathrm{k\Omega\,cm}^2$ is still several orders of magnitude smaller than that of free-standing lipid bilayer ($\sim 1\,\mathrm{M\Omega\,cm}^2$). By comparison with the model that assumes the diffusion of ions across leaky membranes, we conclude that the poor resistance results from the chemical heterogeneity of the oxide.

This work was supported by the German Science Foundation (SFB 563), the Fonds der Chemischen Industrie, EU FP6 (GaNano), and German Federal Ministry of Science and Education (BMBF).

References

1. E. Sackmann, Science **271**, 43 (1996).
2. E. Sackmann, M. Tanaka, Trends Biotechnol. **18**, 58 (2000).
3. M. Tanaka, E. Sackmann, Nature **437**, 656 (2005).
4. A.A. Brian, H.M. McConnell, Proc. Natl. Acad. Sci. U.S.A. **81**, 6159 (1984).
5. G. Steinhoff, O. Purrucker, M. Tanaka, M. Stutzmann, M. Eickhoff, Adv. Funct. Mater. **13**, 841 (2003).
6. P. Bergveld, IEEE Trans. Biomed. Eng. **BM17**, 70 (1970).
7. J. Fritz, E.B. Cooper, S. Gaudet, P.K. Sorger, S.R. Manalis, Proc. Natl. Acad. Sci. U.S.A. **99**, 14142 (2002).
8. A. Poghossian, M.J. Schoning, P. Schroth, A. Simonis, H. Lüth, Sensors Actuators B-Chemical **76**, 519 (2001).
9. P. Fromherz, ChemPhysChem **3**, 276 (2002).
10. H. Hillebrandt, G. Wiegand, M. Tanaka, E. Sackmann, Langmuir **15**, 8451 (1999).
11. O. Purrucker, H. Hillebrandt, K. Adlkofer, M. Tanaka, Electrochim. Acta **47**, 791 (2001).
12. H. Hillebrandt, M. Tanaka, E. Sackmann, J. Phys. Chem. B **106**, 477 (2002).
13. D. Gassull, A. Ulman, M. Grunze, M. Tanaka, J. Phys. Chem. B **112**, 5736 (2008).
14. G. Zeck, P. Fromherz, Proc. Natl. Acad. Sci. U.S.A. **98**, 10457 (2001).
15. M. Tutus, O. Purrucker, Y. Adlkofer, M. Eickhoff, M. Tanaka, Phys. Status Solidi B-Basic Solid State Phys. **242**, 2838 (2005).
16. B. Baur, G. Steinhoff, J. Hernando, O. Purrucker, M. Tanaka, B. Nickel, M. Stutzmann, M. Eickhoff, Appl. Phys. Lett. **87**, 3 (2005).
17. O. Ambacher, J. Phys. D: Appl. Phys. **31**, 2653 (1998).
18. O. Ambacher, M. Eickhoff, A. Link, M. Hermann, M. Stutzmann, F. Bernardini, V. Fiorentini, Y. Smorchkova, J. Speck, U. Mishra, W. Schaff, V. Tilak, L.F. Eastman, Phys. Status Solidi C **0**, 1878 (2003).
19. M. Eickhoff, R. Neuberger, G. Steinhoff, O. Ambacher, G. Müller, M. Stutzmann, Phys. Status Solidi B-Basic Res. **228**, 519 (2001).

20. M. Eickhoff, J. Schalwig, G. Steinhoff, O. Weidemann, L. Görgens, R. Neuberger, M. Hermann, B. Baur, G. Müller, O. Ambacher, M. Stutzmann, Phys. Status Solidi C **0**, 1908 (2003).
21. H. Kim, P.E. Colavita, K.M. Metz, B.M. Nichols, B. Sun, J. Uhlrich, X.Y. Wang, T.F. Kuech, R.J. Hamers, Langmuir **22**, 8121 (2006).
22. G. Steinhoff, M. Hermann, W.J. Schaff, L.F. Eastman, M. Stutzmann, M. Eickhoff, Appl. Phys. Lett. **83**, 177 (2003).
23. B. Baur, J. Howgate, H.G. von Ribbeck, Y. Gawlina, V. Bandalo, G. Steinhoff, M. Stutzmann, M. Eickhoff, Appl. Phys. Lett. **89**, 183901 (2006).
24. G. Steinhoff, B. Baur, G. Wrobel, S. Ingebrandt, A. Offenhausser, A. Dadgar, A. Krost, M. Stutzmann, M. Eickhoff, Appl. Phys. Lett. **86**, 033901 (2005).
25. E. Sabatani, J. Cohenboulakia, M. Bruening, I. Rubinstein, Langmuir **9**, 2974 (1993).
26. H.O. Finklea, D.A. Snider, J. Fedyk, E. Sabatani, Y. Gafni, I. Rubinstein, Langmuir **9**, 3660 (1993).
27. K. Adlkofer, M. Tanaka, Langmuir **17**, 4267 (2001).
28. D. Gassull, S.M. Luber, A. Ulman, M. Grunze, M. Tornow, G. Abstreiter, M. Tanaka, J. Phys. Chem. C **111**, 12414 (2007).
29. F. Cardon, W.P. Gomes, J. Phys. D: Appl. Phys. **11**, L63 (1978).
30. W.P. Gomes, F. Cardon, Prog. Surf. Sci. **12**, 155 (1982).
31. S. Gritsch, P. Nollert, F. Jähning, E. Sackmann, Langmuir **14**, 3118 (1998).
32. C.A. Keller, K. Glasmastar, V.P. Zhdanov, B. Kasemo, Phys. Rev. Lett. **84**, 5443 (2000).
33. R. Richter, A. Mukhopadhyay, A. Brisson, Biophys. J. **85**, 3035 (2003).
34. F.F. Rossetti, M. Bally, R. Michel, M. Textor, I. Reviakine, Langmuir **21**, 6443 (2005).
35. J.P. Dilger, S.G. McLaughlin, T.J. McIntosh, S.A. Simon, Science **206**, 1196 (1979).
36. P. Fromherz, V. Kiessling, K. Kottig, G. Zeck, Appl. Phys. A **69**, 571 (1999).
37. M. Montal, P. Müller, Proc. Natl. Acad. Sci. U.S.A. **69**, 3561 (1972).
38. G. Wiegand, N. Arribas-Layton, H. Hillebrandt, E. Sackmann, P. Wagner, J. Phys. Chem. B **106**, 4245 (2002).
39. J.R. MacDonald, *Impedance Spectroscopy* (John Wiley & Sons, New York, 1987).